Nuclear structure aspects of the heaviest N~Z nuclei south of ^{100}Sn

M. Górska[1], in collaboration with H. M. Albers[1], T. Arici[1], A. Banerjee[1], G. Benzoni[2], A. Blazhev[3], B. Cederwall[4], B. Das[1], T. Davinson[5], J. Gerl[1], H. Grawe[1], O. Hall[5], N. Hubbard[1,6], S. Jazrawi[7,8], J. Jolie[3], M. Mikołajczuk[1,9], A. K. Mistry[1,6], D. Mengoni[10], Zs. Podolyák[7], M. Polettini[2,11], P. H. Regan[7,8], M. Rüdigier[6], A. Yaneva[1,3], J. Vesic[12], G. Zhang[10]

[1] GSI Helmholtzzentrum für Schwerionenforschung GmbH - Darmstadt, Germany
[2] INFN, Sezione di Milano - Milano, Italy
[3] Institut für Kernphysik der Universität zu Köln, D-50937 - Köln, Germany
[4] KTH Royal Institute of Technology - Stockholm, Sweden
[5] University of Edinburgh, School of Physics and Astronomy - Edinburgh EH9 3FD, UK
[6] Institut für Kernphysik, Technische Universität Darmstadt - Darmstadt, Germany
[7] Department of Physics, University of Surrey - Guildford, GU2 7XH, UK
[8] National Physical Laboratory - Teddington, Middlesex, TW11 0LW, UK
[9] Faculty of Physics, University of Warsaw - Warsaw, 00681, Poland
[10] Dipartimento di Fisica e Astronomia, Università di Padova and INFN Padova - Padua, Italy
[11] Dipartimento di Fisica, Università degli Studi di Milano - Milano, Italy
[12] Jozef Stefan Institute - Jamova cesta 39, 1000 Ljubljana, Slovenia

ABSTRACT: Ever-lasting interest in the structure of ^{100}Sn and neighbouring nuclei is still well justified by the fact that it is the heaviest doubly-magic nucleus with N=Z. State-of-the-art experimental techniques involving stable and radioactive beam facilities have enabled access to these exotic nuclei. In particular, the analysis of experimental data obtained in two DESPEC experiments at GSI Darmstadt extends the information on the shell structure and its evolution towards $N = Z = 50$, and allows the study of seniority conservation and proton–neutron interaction in the $g_{9/2}$ orbit. Several theoretical approaches for shell-model investigations are discussed and their predictive power assessed. The calculated systematics of the reduced transition probabilities for high- to medium-spin states in N~Z isotopes with active $g_{9/2}$ orbit is presented for the first time.

Introduction

The repulsive Coulomb force between the protons in the atomic nucleus causes ^{100}Sn, as predicted, to be the heaviest N=Z nucleus that is particle bound in its ground state [1]. Indeed, ^{100}Sn is positioned directly at the proton dripline in the chart of isotopes [2], which makes its direct study extremely challenging caused by low production cross sections for excited states in those nuclei in any kind of known nuclear reaction. It is also the heaviest doubly-magic nucleus with N=Z. The next lighter one is ^{56}Ni, where the softness of the core was discussed extensively in the past and the onset of deformation is exhibited only few nucleons away, as discussed in a recent update [3]. The advantage of the ^{100}Sn region as compared to ^{56}Ni is the increased mass of the core nucleus and therefore its predicted robustness for shell-model studies, as well as the fact that the intruder $g_{9/2}$ orbit (from the N = 4 harmonic oscillator shell) placed just below, is the first high-spin orbital in the shell-model scheme [4]. It requires an additional quantum label in its n-particle wave functions, namely the seniority ν, counting the number of unpaired nucleons for protons and neutron occupying the same shell-model orbital. This particular orbital at the Fermi surface of the nuclei in the region gives rise to isomeric states that often make experimental investigations a little easier. Therefore, as recently reviewed [5], a lot of progress was achieved on ^{100}Sn and its neighbouring nuclei experimentally as well

as from the nuclear structure theory side. In particular, the nuclei south of ^{100}Sn are slightly easier to access and their structure can be categorized as follows. The T=1 coupling of two identical particles in the $g_{9/2}$ leads to the seniority 8^+ isomers as in e.g. ^{98}Cd [6,7,8]. The strength of the πν interaction in the $\pi\nu g_{9/2}$ orbits is manifested in the strongly-binding $T=0(g_{9/2})^2$; $I^{\pi}=9^+$ two-body matrix element (TBME), which is comparable with the T=1 pairing [9, 10]. Indeed, a particular feature of the structure of nuclei south of ^{100}Sn is a large overlap of the proton and neutron wave functions causing an expected strong proton-neutron correlation and creating isospin diminishing coupled pairs (T=0), the so-called isovector coupling, is very attractive. This particlar coupling is responsible for the existence of spin-gap isomers in nuclei in the vicinity of ^{100}Sn. In ^{98}In the first excited state is predicted to be $I^{\pi}=9^+$ similar to that of ^{96}Cd, where the coupling of the two proton neutron pairs to the maximum total angular momentum of $I^{\pi}=16^+$ was identified [11,12]. The identification of excited states in ^{92}Pd [13] provoked an extended discussion in the literature on the πν pairs in the region.
Further significant progress in understanding nuclei in the ^{100}Sn region, as proposed in this work, based on the DESPEC collaboration strategy, is to investigate the structure of intermediate states populated in the decay of isomeric states by lifetime measurements.

Experimental approaches

To populate intermediate- to high-spin states in these neutron deficient nuclei, two methods are most effective and are commonly used. First, fusion-evaporation reactions are best for production of high-spins for prompt and delayed spectroscopy, and second, the fragmentation

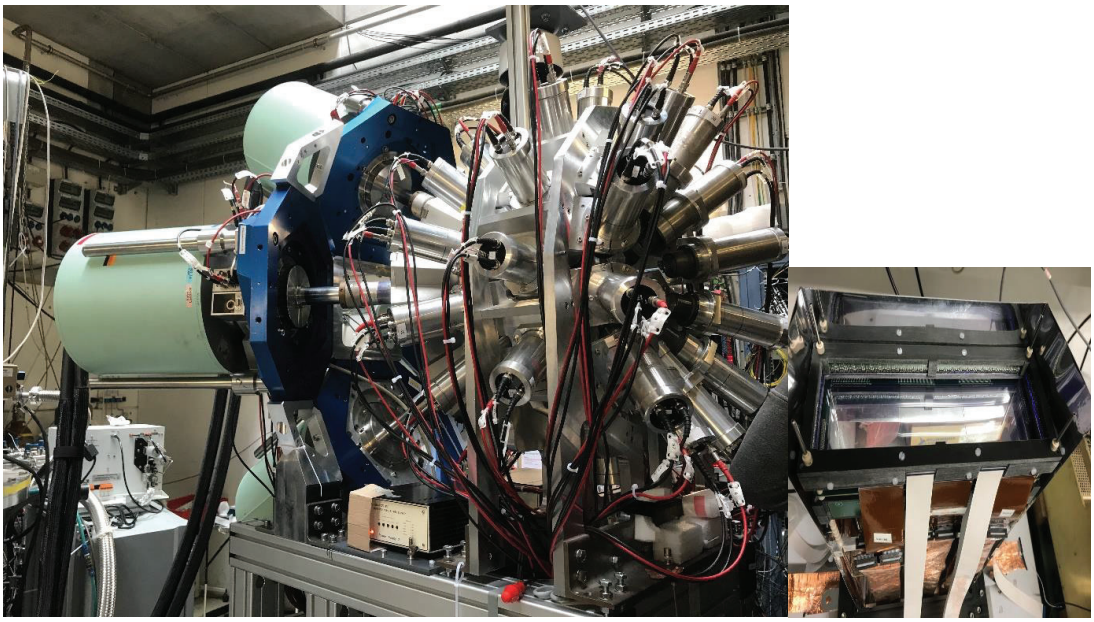

Fig. 1 DESPEC Experimental setup used for decay spectroscopy and intermediate lifetime measurements in the ^{100}Sn region at FAIR Phase-0 at GSI Darmstadt [18]. On the left, γ-ray detectors including the HPGe GALILEO-DEGAS [19] as well as Fatima [20] $LaBr_3$ arrays are shown. On the right the ion-implantation setup consisting of AIDA [21] surrounded by plastic scintillators [18]. The implantation setup is placed inside the γ-ray arrays during the experiment. The sensitivity of the setup to lifetime measurement ranges from tens of picoseconds to tens of seconds (see text for details).

reactions for delayed spectroscopy. The first reaction type has typically much higher cross sections but much lower selectivity of the reaction exit channel such that the nucleus of interest cannot be selected in the data even if produced with larger luminosity than in fragmentation reactions. The latter, if combined with spectrometers such as the FRS [14] at GSI or the BigRIPS [15] at RIKEN, allows for unambigous selection of an exit channel with the transmission through the separator of about 30-50%. In particular, if the state of interest is populated in the decay of an ~μs isomer which can survive the flight path through the separator, it can be exclusively detected in a γ-ray array at the final focal plane.
Recently, multinucleon transfer reactions have also been used to avoid population of an isomer. The selectivity is then also supplied by a spectrometer such as PRISMA [16] or VAMOS [17]. The γ-ray array is then placed at the reaction target. However, this type of reaction does not provide sufficiently-large cross sections for the most neutron deficient nuclei which can only be studied in fragmentation facilities.
The DESPEC experimental setup [18] placed behind the FRS, used for decay spectroscopy and intermediate lifetime measurements in the ^{100}Sn region, is shown in Fig. 1. Two types of γ-ray detectors, the HPGe GALILEO-DEGAS [19] and FATIMA [20] $LaBr_3$ arrays, were exploited to guarantee excellent identification and minimised background as well as very good time resolution for the lifetime measurements. Indeed, the state-of-the-art HPGe detectors suffer from poor time resolution, which largely exceeds the primary limitations of the charge collection time. On the other hand, $LaBr_3$ scintillators exhibit very good energy resolution compared to other scintillating materials, but still poor when compared to HPGe detectors, which results in an exhanced background in the spectra that is not easy to separate. Therefore, a combination of both detector systems is at present the preferred option. The ion-implantation part of the setup consists of AIDA double-sided silicon strip detectors [21] surrounded by plastic scintillators [18]. The implantation setup is surrounded by γ-ray arrays during the experiment.
In particular, for ^{100}Sn region, the existence of two different primary beams that can be delivered by GSI accelerator system - ^{124}Xe and ^{107}Ag - are advantageous to study neutron deficient isotopes with Z>46 and Z<47, respectively, in fragmentation reactions on ^{9}Be targets of 4-8 g/cm^2 thickness. The setup allows for manifold excited states' lifetime measurements. Single hit γ-ray spectra can be constructed directly within 20μs from the implantation time, and through time stamps, up to a value that is only naturally limited by the implantation rates. The double-fold γ-ray coincidences allow for lifetime measurement of intermediate states using various analysis procedures from tens of picoseconds to several μs [18].

Results

Two DESPEC experiments were performed to date that address the structure in the ^{100}Sn region. In the first one, as already preliminarly reported [22, 23, 24], the isomeric decays in ^{94,96}Pd have been measured. This data is in the final analysis stage and will be submitted for a final publication soon [25]. The results will include verification of lifetimes of intermediate spin states below the $I^{\pi}=8^{+}$ isomer in ^{96}Pd [26] with an improved accuracy. Moreover, the recently reported lifetimes in ^{94}Ru [27] caused a polemic in the literature as an in-beam experiment presented a disagreement with the reported value [28]. Therefore, those measurements call for a further verification. The newest result of our rich data set of the first experiment are the lifetimes of intermediate states below the $I^{\pi}=21/2^{+}$ in ^{95}Rh [29].
From the second experiment, lifetimes of excited intermediate states populated in the isomeric decays in ^{98,100}Cd, as well as in ^{102}Sn, will be reported soon [30]. The lifetime measurement of the first excited state in ^{103}Sn was also one of the goals of this experiment. The experimental data is in the final analysis stage. The γ-ray spectrum measured with the HPGe detector array within 2.3μs after implantation of ^{98}Cd is shown in Fig. 2, where the known gamma transitions

[6] are indicated. This spectrum demonstrates that the collected data is not disturbed by any contaminants, and the selected ion identification condition could therefore be used for further analysis with the FATIMA array.

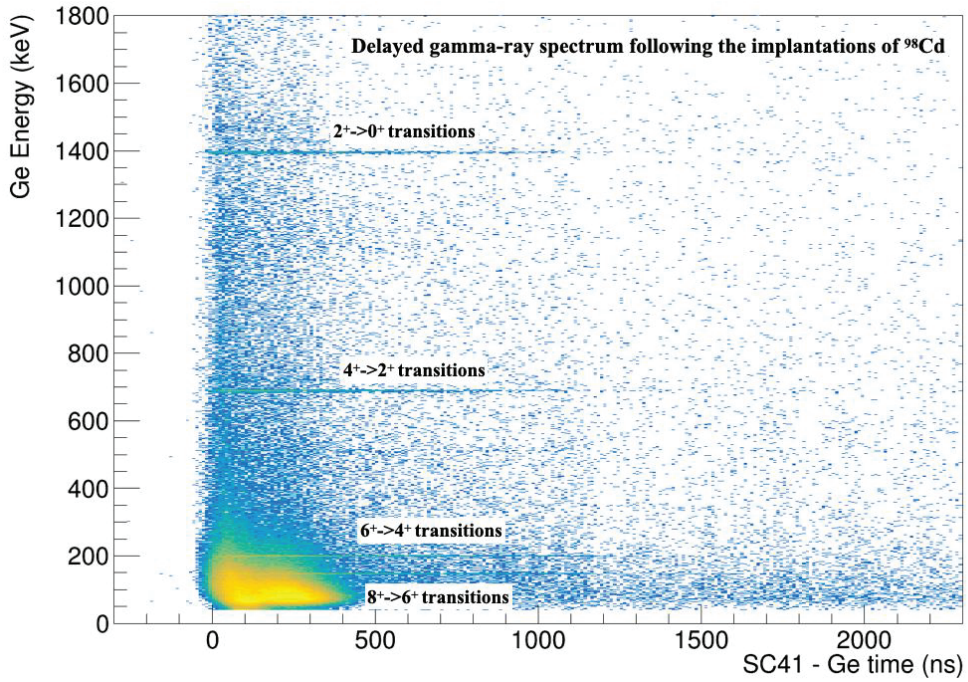

Fig.2 Delayed γ-ray spectrum obtained in the HPGe-array in the DESPEC experiment vs time of the γ-ray detection after ^{98}Cd implantation. The indicated transitions correspond to the known γ rays [6].

Interpretation scope and predictions

The motivation for the lifetime measurement, as mentioned before, is the evolution of the shell structure from the doubly-magic ^{100}Sn towards the mid shell for protons and neutrons where the spectrum of ^{88}Ru indicates a rotational band [31]. The approach is to understand first the N=50 isotopes, verifying our understanding of their structure. The next step would employ the study of N=48 isotones to observe and judge the contribution of the neutron wave functions, which will further increase towards N=Z nuclei as the collectivity increases. This is observed for 4 neutrons in the $g_{9/2}$, in ^{88}Ru, in contrast to the ^{96}Cd N=Z nucleus.
In Ref. [32] predictions using large model spaces $\pi\nu(f_{5/2}pg_{9/2})$ and $\pi\nu$(sdg) are compared to a pure $g^n_{9/2}$ approach for B(E2) values and spectroscopic quadrupole moments in ^{92}Pd and ^{96}Cd. In the low-spin range I ≤6 the three approaches are equivalent for excitation energy and B(E2) values, but exhibit large differences in the spectroscopic quadrupole moments, which are not experimentally accessible at present. This is expected to change for higher spin and closer to the magic numbers N=Z=50 due to model space exhaustion. In Fig. 3, reduced transition strength calculations are shown for even ^{92,94,96}Pd isotopes and for even ^{96,98}Cd isotopes in the upper and lower panels, respectively. The single $g_{9/2}$ orbital model space was considered using the interaction from Ref. [33]. For the cases of ^{100}Cd shown in the lower panel as well, the MHJM [34] interaction was used. Standard effective charges of e_π=1.5e and e_ν=0.5e were used for the $g_{9/2}$ shell calculation, while e_π=1.49e and e_ν=1.4e charges were used for MHJM interaction [35].

It is indeed obvious from Fig. 3 that reduced "collectivity", exhibited here in the lowering B(E2) values, in ^{92}Pd towards higher spin is caused by the limited model space used in this calculation. The existence of the $I^{\pi}=16^{+}$ spin gap isomer in ^{96}Cd does not allow the same conclusion to be drawn, and therefore the future lifetime measurement of the $I^{\pi}=8^{+}$ state will allow the question of $\pi\nu$ coupling in this nucleus to be answered. The collected data on ^{94}Pd may shed light on this problem as this nucleus is situated at a critical point of this evolution. It is the even-even neighbour of the difficult to access N=Z ^{92}Pd, ^{96}Cd and ^{94}Ag nuclei. The ^{94}Pd spectrum represents the T=1 partner of ^{94}Ag. With respect to seniority, ^{94}Pd reflects with ν_{π}=2,4, ν_{ν}=2 the transition from $\nu_{\pi} = \nu_{\nu}$=2,4 ^{92}Pd to $\nu_{\pi} = \nu_{\nu}$=2 ^{96}Cd with an intermediate B(E2; I → I - 2) pattern in $g^{n}_{9/2}$ [32] (see Fig. 3).
Similarly, ^{94}Pd is an intermediate case of ^{92}Pd and ^{96}Pd showing an increasing role of valence neutrons. The experimental results and discussion of transition strengths with larger model spaces for this nucleus are planned in aforthcoming paper [25].

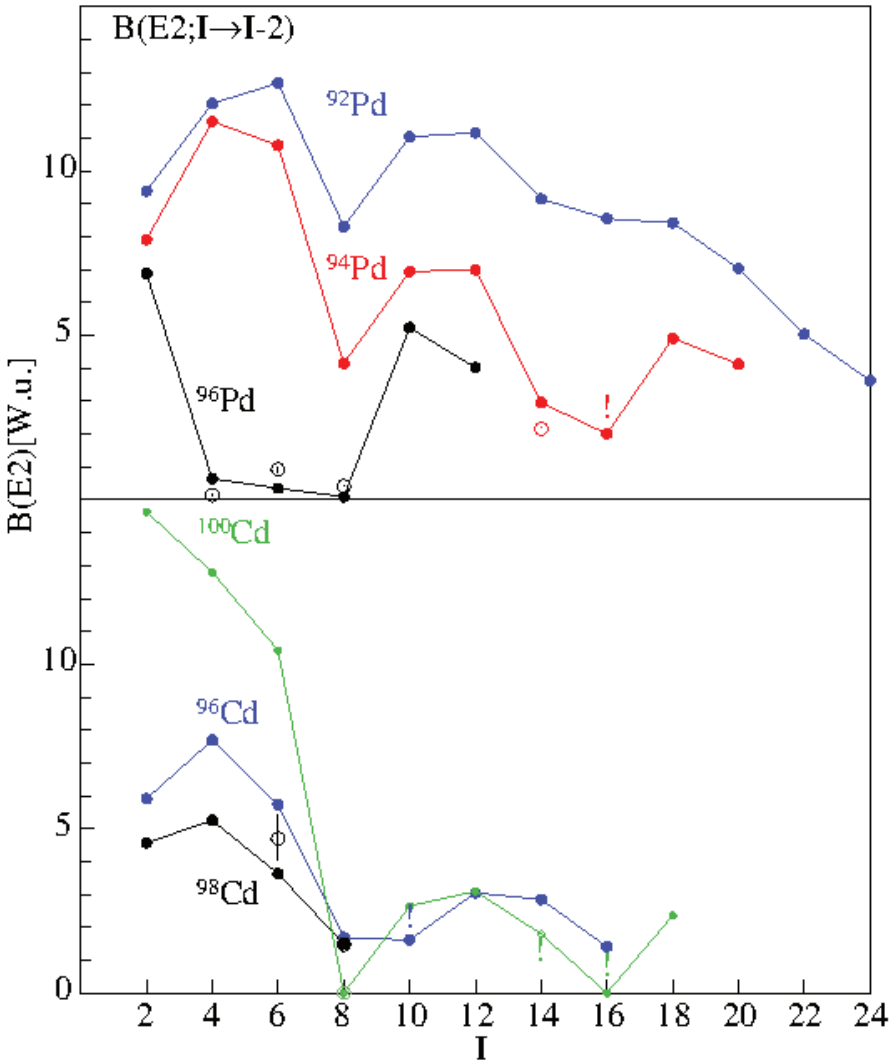

Fig.3. Shell model I → I -2 B(E2) strengths in a pure $\pi\nu g_{9/2}$ space [33] for the yrast states in even Pd isotopes in the upper panel and even Cd isotopes (lower panel). B(E2) values marked by "!" can not be observed because of a competing I→I-1 M1 or other transition. The reduced transition strengths in ^{100}Cd is

calculated using MHJM interaction [34]. The experimental values known in ^{94}Pd [8], ^{96}Pd [8,26], ^{98}Cd [8], ^{100}Cd [36] are represented with the coloured circles with the corresponding error bars, which are in some cases smaller than the size of the symbols.

The evolution of the E2 transition strength in Cd isotopes shown in Fig. 3 has a different background. As already mentioned, the $I^{\pi}=8^{+}$ seniority remnant of that isomer in ^{98}Cd (and predicted in ^{98}Sn) is expected in ^{96}Cd except of the strongly-bound $I^{\pi}=16^{+}$ spin-gap isomer. In contrast, the known $I^{\pi}=8^{+}$ isomer in ^{100}Cd [37] is interpreted as a drastic configuration change from pure (in this model space) proton state to the first $I^{\pi}=6^{+}$ state dominated by the neutron wave function originating from the $I^{\pi}=6^{+}$ isomer in ^{102}Sn. Certainly, also the second, proton wave function dominated $I^{\pi}=6^{+}$ state is present close in energy to the first one. The amount of mixture of the $6^{+}_{1,2}$ states, governed by the πν interaction between the shell below and above ^{100}Sn, can be elaborated based on the lifetime measurements of those states. The small value for the B(E2:$16^{+} \rightarrow 14^{+}$) in Fig. 3 is related to the involvement of the $h_{11/2}$ orbital as the state appears at an excitation energy of ~10 MeV and has multiple other decay possibilities. The situation changes drastically when removing another 2 protons from ^{100}Cd: ^{98}Pd develops significant collectivity already in low-spin states, as known from the literature [38], even if a slight reduction of the transition strength is still predicted for the $I^{\pi}=8^{+}$ which is also reflected in the longer lifetime measured for this state.

Conclusions

^{100}Sn being the heaviest doubly-magic self-conjugated nucleus provides unique opportunity to study the in-medium πν interaction with respect to that heavy core. There are multiple phenomena associated to the intermediate spin states, which are then overtaken by the on-set of collectivity if enough particles are contributing to the wave function. Exactly that critical point is decisive to be traced. Therefore, it is of great interest to know the lifetimes of intermediate states in this region of nuclei. Only state-of-the-art accelerators and detector development allow for accessing some of them already now.

[1] Dobaczewski J , Nazarewicz W, 1995 *Phys. Rev.* C **51**, R1070
[2] Faestermann T, Górska M, and Grawe H, 2013 *Prog. Part. Nucl.Phys*. **69**, 85-130
[3] Arnswald K et al., 2021 Phys. Lett. **B 820** 136592
[4] Zamick L, 2016 Phys. Rev. C **93**, 034327
[5] Górska M, 2022 *Physics 4*(1).
[6] Górska M et al., 1997 *Phys. Rev. Lett.* **79**, 2415
[7] Blazhev A et al., 2004 Phys. Rev. C **69**, 064304
[8] Park J et al., 2017 *Phys. Rev*. C **96** 044311, and erratum: 2021 *Phys. Rev*. C **103** 049910
[9] Serduke F J D, R. Lawson L, and Gloeckner D H, 1976 *Nucl. Phys*. **A 256**, 45
[10] Gross R and Frenkel A, 1976 *Nucl.Phys*. **A 267**, 85
[11] Nara Singh B S, et al. 2011 *Phys.Rev.Lett.* **107**, 172502
[12] Davies P J et al., 2019 *Phys. Rev*. C **99**, 021302(R)
[13] Cederwall B et al., 2011 *Nature* **469**, 68
[14] Geissel H et al., 1992 *Nucl. Instr. Meth*. **B 70**, 286
[15] Kubo T et al., 2012 *Prog. Theor. Exp. Phys*. 03C003
[16] Stefanini A M et al., 2002 *Nucl. Phys.* **A 701** 217
[17] Pullanhiotan S et al., 2008 *Nucl. Instr. Meth.* **B 266**, 4148
[18] Mistry A K et al., 2022 *Nucl. Inst. Meth.* **A 1033**, 166662
[19] Li G S, 2018 *Nucl. Instrum. Meth.* **A 890**, 148

[20] Rüdigier M et al., 2022 *Nucl. Instr. Meth.* **A 969**, 163967
[21] Technical Report For the Design, Construction and Commissioning of the Advanced Implantation Detector Array (AIDA) (2018), https://edms.cern.ch/ui/#!master/navigator/document?D:100356483:100356483:subDocs

[22] Jazrawi S et al., 2022 *Radiation Physics and Chemistry* 200, 112234
[23] Polettini M et al., 2021 Il Nuovo Cimento 44 C 67
[24] Yaneva A et al., *Zakopane Conf. Nucl. Phys.* 2022, in preparation
[25] Yaneva A et al., in preparation
[26] Mach H et al., 2017 *Phys. Rev.* C **95**, 014313
[27] Das B et al., 2022 *Phys. Rev.* C **105**, L031304
[28] Pérez-Vidal R M *et al.* 2022 *Phys. Rev. Lett.* **129**, 112501
[29] Das B. et al., submitted
[30] Zhang G et al., to be published
[31] Cederwall B et al., 2020 *Phys. Rev. Lett.* **124**, 062501
[32] Zuker A, Poves A, Nowacki F, and Lenzi S, 2015 *Phys.Rev.* C **92**, 024320
[33] Coraggio L, Covello A, Gargano A, and Itaco N, 2012 *Phys.Rev*. C **85**, 034335
[34] Kavatsyuk O, et al., 2007 *Eur. Phys. J*. **A 31**(3) 319, and Blazhev A, Górska M, Grawe H in preparation
[35] Grawe H, et al., 2021 *Phys. Lett*. B 820, 136591
[36] NNDC National Nuclear Data Center, NuDat 3. Available online: https://www.bnl.gov/world/ (accessed on November 2022)
[37] Górska M et al., 1994 Z. Phys. **A 350**, 181
[38] Fransen C, et al., 2009 AIP Conference Proceedings **1090**, 529